Author's Accepted Manuscript

Glare, a GIS tool to reconstruct the 3D surface of palaeoglaciers

Ramón Pellitero, Brice R. Rea, Matteo Spagnolo, Jostein Bakke, Susan Ivy-Ochs, Craig R. Frew, Philip Hughes, Adriano Ribolini, Sven Lukas, Hans Renssen

Cite this article as: Ramón Pellitero, Brice R. Rea, Matteo Spagnolo, Jostein Bakke, Susan Ivy-Ochs, Craig R. Frew, Philip Hughes, Adriano Ribolini, Sven Lukas and Hans Renssen, Glare, a GIS tool to reconstruct the 3D surface of palaeoglaciers, *Computers and Geosciences* http://dx.doi.org/10.1016/j.cageo.2016.06.008

This is a PDF file of an unedited manuscript that has been accepted for publication. As a service to our customers we are providing this early version of the manuscript. The manuscript will undergo copyediting, typesetting, and review of the resulting galley proof before it is published in its final citable form. Please note that during the production process errors may be discovered which could affect the content, and all legal disclaimers that apply to the journal pertain.

GlaRe, a GIS tool to reconstruct the 3D surface of palaeoglaciers

Ramón Pellitero*[1], Brice R. Rea[2], Matteo Spagnolo[3], Jostein Bakke[4], Susan Ivy-Ochs[5], Craig R. Frew[6], Philip Hughes[7], Adriano Ribolini[8], Sven Lukas[9], Hans Renssen[10].

1. Department of Geography and Environment. University of Aberdeen. St Mary's, Elphinstone Road. AB24 3UF Aberdeen (United Kingdom). r.pellitero-ondicol@abdn.ac.uk

* Corresponding author

2. Department of Geography and Environment. University of Aberdeen. St Mary's, Elphinstone Road. AB24 3UF Aberdeen (United Kingdom). b.rea@abdn.ac.uk

3. Department of Geography and Environment. University of Aberdeen. St Mary's, Elphinstone Road. AB24 3UF Aberdeen (United Kingdom). m.spagnolo@abdn.ac.uk

4. Department of Earth Science. University of Bergen, P.O.Box 7800 5020 Bergen (Norway). Jostein.Bakke@geo.uib.no

5. Insitut für Teilchenphysik, ETH-Höggerberg. Otto-Stern-Weg 5, 8093 Zürich Switzerland. ivy@phys.ethz.ch

6. craigrfrew@gmail.com

7. Geography, School of Environment, Education and Development, University of Manchester, Oxford Road, Manchester M13 9PL (United Kingdom). Philip.Hughes@manchester.ac.uk.

8. School of Geography, Queen Mary, University of London. Mile End Road London E1 4NS (United Kingdom). s.lukas@qmul.ac.uk

9. Dipartimento Scienze della Terra - Università di Pisa - Via S. Maria 53 - 56126 Pisa.ribolini@dst.unipi.it

10. Department of Earth Sciences, Faculty of Earth and Life Sciences, VU University Amsterdam, Netherlands. h.renssen@vu.nl

Abstract:

Glacier reconstructions are widely used in palaeoclimatic studies and this paper presents a new semi-automated method for generating glacier reconstructions: GlaRe, is a toolbox coded in Python and operating in ArcGIS. This toolbox provides tools to generate the ice thickness from the bed topography along a palaeoglacier flowline applying the standard flow law for ice, and generates the 3D surface of the palaeoglacier using multiple interpolation methods. The toolbox performance has been evaluated using two extant glaciers, an icefield and a cirque/valley glacier from which the subglacial topography is known, using the basic reconstruction routine in GlaRe. Results in terms of ice surface, ice extent and equilibrium line altitude show excellent agreement that confirms the

robustness of this procedure in the reconstruction of palaeoglaciers from glacial landforms such as frontal moraines.

1. Introduction

The existence and dimensions of terrestrially terminating glaciers is controlled, to a first order, by climate, through variations in temperature and precipitation (Ohmura et al., 1992). The Equilibrium Line Altitude (ELA) of a glacier is the key glacier surface location where empirical relationships relating these two climatic parameters have been determined (Ohmura et al., 1992; Braithwaite, 2008). The ELA is the elevation on the glacier where, at the end of the ablation season, the net mass balance is zero (i.e. snow and ice melted equals snow and ice accumulated within one year). ELAs can be calculated on present-day glaciers by making surface mass balance measurements (measured or geodetic) and can also be determined for palaeoglaciers using various techniques, most of which require knowledge of some component of the glacier geometry (Pellitero et al., 2015). Once a palaeoglacier ELA has been established, either the temperature or precipitation relating to it can be determined, providing quantitative palaeoclimate information for that location (Hughes and Braithwaite, 2008). Given the importance of the ELA for palaeoclimatology especially in high latitudes and altitudes, a rigorous reconstruction of the 3D geometry of the palaeoglacier is essential (e.g. Carr et al., 2010).

Palaeoglacier surface and volume reconstruction methods rely on morphological evidence of the former glacier geometry (e.g. terminal and lateral moraines, lateral meltwater channels, trimlines, kame terraces and ice contact deltas), to either initiate (iterative) or constrain (dynamical) the model (Federici et al., 2008; Lukas, 2006; Pellitero, 2013; Rea and Evans 2007). Ideally, there would be a wealth of landform evidence available for the reconstruction but in reality, most landforms are missing or fragmentary, especially in the accumulation zone, and often become increasingly degraded with age (e.g. Dawson, 1979). The best practice is therefore to use the available landform evidence in combination with numerically derived reconstructions. These numerical approaches are rooted in the constitutive equations for glacier motion (Nye, 1952a, b) and create an equilibrium glacier profile over the known, former, subglacial bed. This approach makes three assumptions:

1. the present-day topography is the same as the palaeoglacier basal topography. Evidence of considerable post-glacial geomorphological activity by proglacial, periglacial, paraglacial, fluvial and/or mass movement processes (e.g. infilled lakes or large mass movements) should be taken into consideration, and where possible, the present-day topography corrected.
2. the reconstructed glacier was in equilibrium with climate.
3. the palaeoglacier was land terminating. Calving impacts on the mass balance via geometrical and mass flux changes.

This paper presents a GIS tool that semi-automatically reconstructs the 3D geometry for palaeoglaciers given the bed topography. The tool utilises a numerical approach and can work using a minimum of morphological evidence (i.e. the position of the palaeoglacier front or tuned to a lateral moraine or trimline). The numerical approach is based on an iterative solution to the perfect plasticity assumption for ice rheology, explained in Benn and Hulton (2010). The tool can be run in ArcGIS 10.1 (ArcInfo license) and later updates and the toolset is written in Python code.

2. Perfect Plasticity Rheology

The model implemented in GlaRe produces an equilibrium profile of a glacier in two dimensions (i.e. along the central flowline). The model takes no account of basal sliding, and it assumes that ice has a perfect plasticity rheology (Paterson, 1994, p. 240). It is based on the Shilling and Hollin (1981) formula:

$$(1) \qquad h_{i+1} = h_i + \frac{\tau_{av}}{F_i \rho g} \frac{\Delta x}{H_i}$$

where, h is ice surface elevation, τ_{av} is basal shear stress (in Pa), F is a shape factor, ρ is ice density (~900 kg m^{-3}), g is the acceleration due to gravity (9.81 ms^{-2}), Δx is step length (in metres), H is ice thickness (in metres), and i refers to the iteration (step) number. This is a derivation from the well-known Nye (1952a) formula for the calculation of shear stress at the base of a glacier

$$(2) \qquad \tau = \rho g H \sin\alpha$$

where, τ is the basal shear stress, and α is the ice surface slope.

Equation 1 does not have a solution at the snout of the glacier, because τ_i and τ_{av} are equal to 0. Van der Veen (2013) solved this shortcoming by evaluating the ice thickness and the shear stress at the midpoint along iterative steps. The result is Equation 3, which can be solved as a quadratic equation. The complete explanation and development of these formulae can be found in Benn and Hulton (2010) and Van der Veen (2013).

(3)

$$h_{i+1}^2 - h_{i+1}(b_i + b_{i+1}) + h_i(b_{i+1} - H_i) - \frac{2\Delta x \overline{\tau_0}}{Fg} = 0$$

where, b is the bed elevation.

In this paper we present a GIS tool that utilises this numerical approach to reconstruct the geometry of former, land-terminating glaciers, provided that the position of their frontal moraine or ice margin is known. It is particularly suited to the reconstruction of cirque and valley glaciers. However, it can also be successfully used for plateau-fed glaciers and small ice caps/fields. The GIS tool allows users to define three input parameters – the basal shear stress (τ) , the shape factor (F) and the interpolation procedure. These inputs are discussed further below.

2.1. Basal shear stress τ

The model requires the glacier basal shear stress as a primary input because this parameter exerts a first-order control on the output glacier 3D surface. Field and experimental data indicate that τ should lie in the ~50-150 kPa range (Nye, 1952b) for a valley glacier (Paterson, 1970) and up to 190 kPa for a cirque glacier (Weertman, 1971). The ideal situation is to initially reconstruct the ice surface using a standard value of 100 kPa and then tune τ to fit the reconstructed 3D glacier surface to the geomorphological constraints on vertical ice thicknesses (e.g. lateral moraines and/or trimlines) (Benn and Hulton, 2010; Schilling and Hollin, 1981). However, these landforms are seldom present or difficult to identify and generally not easy to link to a specific frontal moraine. In the

absence of any constraining geomorphology for palaeoglacier thickness, the standard reference value of 100 kPa for valley glaciers (Paterson, 1994; Rea and Evans, 2007) is recommended and is the default for the tool. Shear stress may not be uniform along the length of a glacier because of bed changes along the flowline (e.g. a change in bedrock lithology/roughness, sediment cover across the valley floor or the decrease of shear stress near the ice divides of plateau icefields/ice caps, see section 3.2). Therefore, experienced users are also given the option to manually alter the shear stress at any point along a flowline.

2.2. Shape factor (F factor).

The Nye (1952a) formula assumes that all the glacier driving stress is supported by the basal shear stress. This is unrealistic for valley glaciers and other topographically constrained glaciers (Benn and Hulton, 2010; Nye, 1952b; Shilling and Hollin, 1981). In these cases, significant resistance to flow can also be provided from lateral-drag, which can be incorporated into the formula using a shape friction factor (F factor).

The concept of F factor was first introduced by Nye (1952b), who suggested it to be a function of the cross-sectional area and perimeter length (equivalent to the wetted perimeter of a river). The F factor was further discussed by Nye (1965), who reduced it to a function of the glacier width and thickness, for simple cross-sectional geometries:

$$W = \frac{w}{H} \qquad (4)$$

Where, for any cross-section, W is a shape-factor indicator, w is half the width of the glacier and H is the centre line ice thickness. W values are converted to the relevant F factor value using conversion tables (Li et al., 2012; Nye, 1965; Paterson, 1994, p. 269). However, W is an approximation of the true shape factor, as the calculation is based on simplified valley cross-sections (i.e. parabolic, semi-ellipse or rectangular). The original F factor is both a more sophisticated and geometrically correct approach and is the preferred method. It utilises the cross-sectional area and perimeter (Shilling and Hollin, 1981). If we extend Equation 2 to the glacier perimeter at a glacier cross-section we find that

$$\tau = \rho \, g \, A \, \sin\alpha \qquad (5)$$

where, A is the cross-section area. Assuming the driving stress is equal to the basal shear stress at the centre line, then the F factor is calculated by the following formula,

$$F = \frac{A}{Hp} \qquad (6)$$

where, H is the ice thickness at a point and p is the length of the cross section ice-bed contact.

This is the approach taken by Benn and Hulton (2010) and implemented in the reconstruction tool here. The F factor, as defined in (6), should be equal to 1 for icecaps and icefields, where there are plateau source areas or poorly defined valley heads, as the driving stress here is entirely supported by basal shear stress (i.e. they are not topographically constrained). However, its value is reduced

considerably, and can have a fundamental impact on the reconstructed ice thickness, where valley constrictions are present (Nye, 1952b). The tool can derive F factors for automatically generated, or user-defined, cross-sections.

2.3. Palaeoglacier DEM interpolation.

The reconstructed equilibrium glacier profile, derived from equation (1) and adjusted by the F factor generates a 2D representation (i.e. the first tool output is a series of ice thickness values along the glacier flowline). In order to calculate a paleo-ELA the 3D geometry of the glacier is required and specifically the hypsometry. The 2D ice thickness flowline data need to be extrapolated to generate the 3D surface. This presents a typical GIS interpolation problem, which can be dealt with using several solutions including "Topo to raster", "Inverse Distance Weighted (IDW)", "Kriging" and "Trend", all available options in the tool. Given the importance of this step for the reconstructed palaeoglacier surface, brief details are provided below.

The Topo to Raster tool interpolates a surface, using an iterative method, which calculates grids at progressively finer scales (Hutchinson 1989). This approach creates smooth, continuous surfaces passing through all the input points. The tool works even for sparse and irregularly spread input points and is more computationally-efficient than other methods (Hutchinson, 1989). The main drawback, with regards to the glacier reconstruction, is that this interpolation is designed to produce a hydrologically correct surface, which is not the case for a glacier surface. As a result, unrealistic concavities can appear if the interpolation is based on ice thickness points located only along one, or very few, glacier flowlines. The number of iterations is also key to this tool, as more iterations will result in a smoother surface (Hutchinson et al., 2011). In the tool, this has been set to an optimum of 20 iterations, following recommendations from Hutchinson et al. (2011).

The IDW is one of the simplest interpolation methods. It is deterministic, which means that surfaces are interpolated depending purely on their distance from the given points. This is based on Tobler's first law of geography (Tobler, 1970): nearer things are more alike than ones further away. This method is exact (the interpolated surface "passes through" all input points), but is unable to model values higher that the input ones, and is very prone to the creation of spurious sinks. The glacier reconstruction tool incorporates a key IDW parameter that enhances or diminishes the influence of nearer points in the interpolation, called "power". This parameter is set to a default value of 2. In practice, a parameter larger than 2 will create a rougher surface (nearer values are more important) and conversely a lower value will create a smoother surface.

The Kriging method is a geostatistical procedure, which means that not only the distance to input points, but also the statistical relationships between the input point values, are taken into account. Kriging requires the use of a larger quantity of input parameters, all having potentially a significant impact on the final result. These should ideally be defined through previous exploratory work of the input data. A complete explanation and guide on kriging can be found in Oliver and Webster (2014). The glacier reconstruction tool implements an ordinary kriging routine, with a spherical model semivariogram whose parameters are calculated by default, and a variable radius with 5 elements, the minimum for interpolation. This means that the interpolation will be made with at least 5 points, no matter how far apart they are.

Trend is an inexact interpolation method. This means that the resulting surface does not need to pass through the initial input points. It is a computationally-fast interpolation method and requires very few input parameters. This method simply fits a linear or polynomial equation so the Root Mean Standard error is minimised. The only parameter is the order of the equation that will calculate the surface. By trialling this method it has been determined that lower errors occur for the quadratic and cubic functions, with errors increasing from the quartic equation degree upwards, especially for areas far from the input points. The tool applies the cubic equation by default, which results in a smooth glacier surface.

Any interpolated surface, no matter what the chosen method, improves with the density of input points. Thus, the more ice thickness flowlines that are generated the better. Once ice thickness points have been derived, and before the glacier surface is interpolated, the tool will generate additional ice thickness points, at set distances, orthogonal to the flowline (using a GIS buffer technique), allocating them the same ice surface elevation as their closest flowline point (see section 3.4). The tool is unable to replicate the effect of submergent and emergent velocities which create the typical concave and convex surfaces of the accumulation and ablation areas. However, our tests on extant valley glaciers (see section 5) suggest that the error in both volume and surface area due to this limitation is minor and the effect on the resulting ELA is minimal.

3. Tool use

GlaRe runs in ArcGIS 10.1 and subsequent updates. It is written in Python 2.7, and primarily uses arcpy and numpy Python libraries, which are automatically installed alongside ArcGIS software. An ArcInfo/Advanced ArcGIS for Desktop license is required, comprising 3DAnalyst and Spatial Analyst. The tool can be downloaded from the Computers and Geosciences GitHub repository at https://github.com/cageo/Pellitero-2015 or from the Younger Dryas research group page at the University of Aberdeen website: http://www.abdn.ac.uk/geosciences/departments/geography-environment/outcomes-442.php. GlaRe has to be imported into the user's ArcToolbox and it consists of five "Toolsets" (Figure 1).

For GlaRe to work properly all input rasters and feature classes should be in the same projection. There are different ways of generating a 3D Surface, depending on the requirement of different parameters discussed in section 2 and the presence, or not, of an extant glacier in the catchment. As shown in Figure 2 there is a simple central path which goes from a user defined flowline and rough glacier limit (typically the catchment where the glacier developed) into the ice thickness retrieval and the 3D surface calculation. But also there are several additional toolsets that will improve the final result by tuning some of the parameters discussed in section 2, such as the glacier basal shear stress or the F factor along the flowline. Also, the toolbox provides a basic tool to remove any extant glacier from the flowline. A detailed guide on the toolset use, with a real example of glacier reconstruction from the inputs provided in the ferrere.mpk file, and some important tips for optimal performance, can be found in Appendix 1.
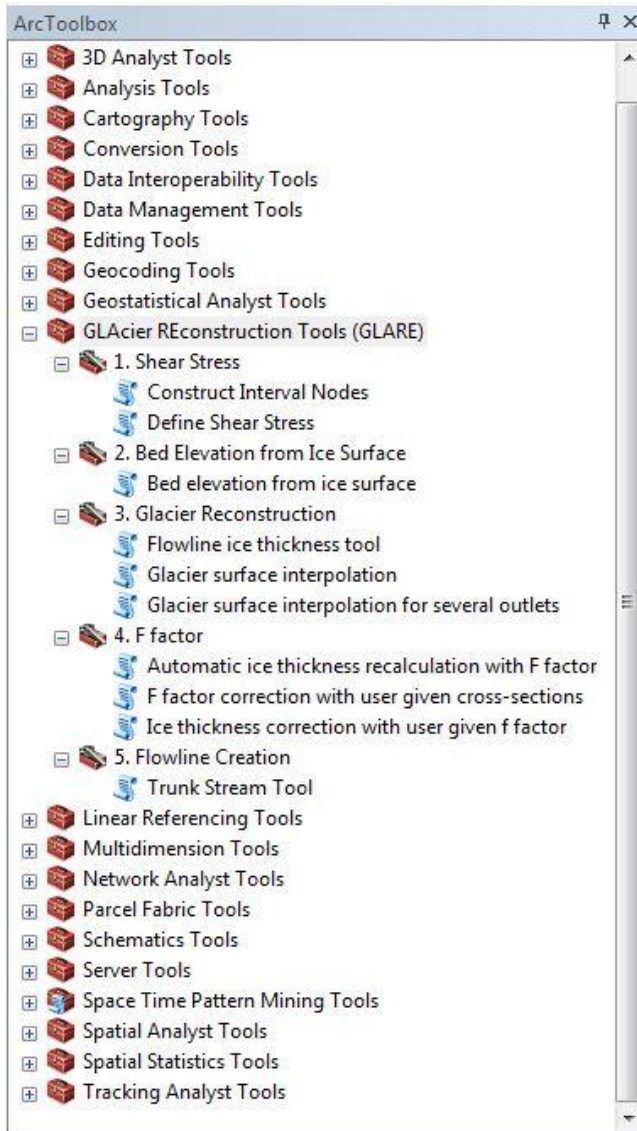
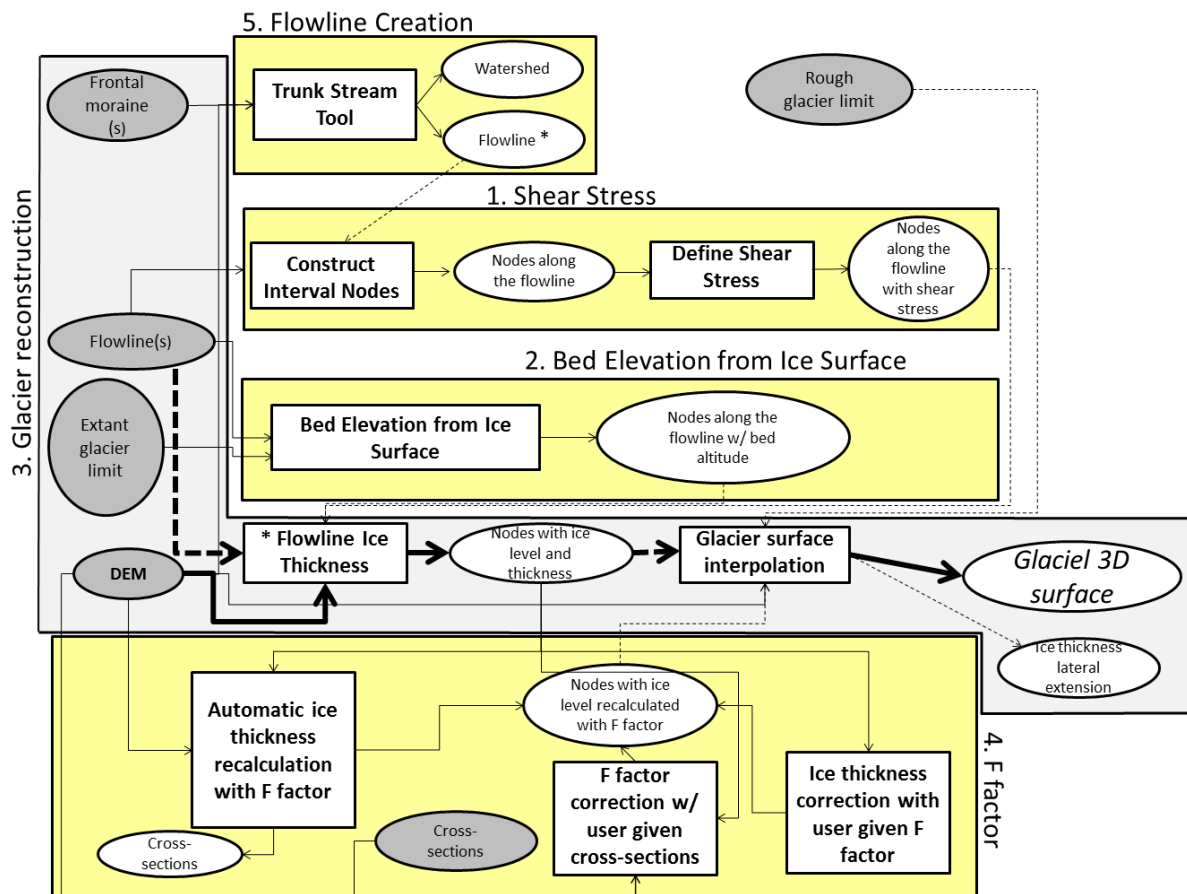Figure 1. GlaRe as it appears in ArcToolbox.

Figure 2. Diagram showing the use of GlaRe. Grey circles are user defined inputs, white squares are tools and white circles are outputs. Plain lines are necessary unique inputs or compulsory outputs, depending on their position in relation to the tool they relate to; dashed lines refer to different possible inputs and optional outputs. The main, most straightforward, path is signed with coarser arrows, and additional toolsets are inset within the yellow colour boxes.

4. Tool testing

Tool's performance has been tested against two different types of present-day glacier where the subglacial bed topography is known: the Folgefonna icefield in Western Norway and the Griesse valley glacier in the Swiss Alps. The aims of these tests were to verify that the tool can replicate the extant glaciers in terms of ice thickness, area, volume and that the ELA determined via the reconstruction tool is comparable to that measured present-day. Given that valley glacier systems are topographically well constrained, the test was run using only the frontal position of the Griesse Glacier along with the subglacial topography as inputs. However, in the much more complex case of an icefield with multiple outlet glaciers, the present-day margin of Folgefonna was used. For both glaciers, three scenarios were tested: (i) no F factors, (ii) use of automatic F factor tool and (iii) calculation of F factor from user-defined cross-sections. In the latter case, the F factor, usually obtained from cross-sections at valley constrictions, is propagated upstream until the topographic constraint terminates (i.e. the icefield reaches a plateau) or the valley geometry changes and a new F factor is calculated, following Rea and Evans (2007).

The Folgefonna glacier consists of three separate plateau icefields covering an area of 207 km^2 with the glacier Sørfonna being the biggest, with a total surface area of 167 km^2. Our target is the northern plateau glacier named Nordfonna with a total ice covered area of 24.47 km^2 and an elevation range from 955 m up to ~1640 m. In total there are five larger outlet glaciers draining the plateau with the largest entering into Lake Juklavatnet on the west side of Nordfonna. During the winter of 2008 and 2009 an extensive radar survey was conducted over the entire glacier with ground penetrating radar using two different frequencies. In total 150 line km were collected using a 5 MHz antenna and 280 line km using a 25 MHz antenna, giving a spatial resolution of the subglacial terrain of 250 m. (5 MHz) and 80 m. (25MHz) (Bakke et al., in prep.). Dual frequencies were used in order to capture high-resolution data in both the deeper and the shallower parts of the glacier. Based on the survey, the total volume of the glacier was calculated as 2387 billion cubic meters. As the plateau glacier is not particularly thick the subglacial topography has a major influence in ice drainage and needs be taken into account when the flow lines are designed. Most of the ice in the northern ice body drains through the outlet glacier Juklavassbreen. A significant amount of ice flows in the opposite direction, eastwards to Vikebygd. The centre of the glacier is drained through a trough that has two opposite outlets on the W and E, although the eastern one seems to dominate in ice drainage towards Raundalsvatnet. Finally the southernmost part seems to host stagnant ice, with only some marginal drainage to the SW, towards the Svartedalsvatnet. The steep W-E precipitation gradient and wind re-distribution of snow (Dahl and Nesje, 1992) plays a significant role in accumulation. Irrespective of the mass balance enhancements the surface slope controls ice drainage direction.

Four main flowlines were created, mirroring the present-day drainage system, extending back to the central ice divide. Several secondary shorter flowlines were also created, accounting for smaller outlets of the icefield (Figure 3).
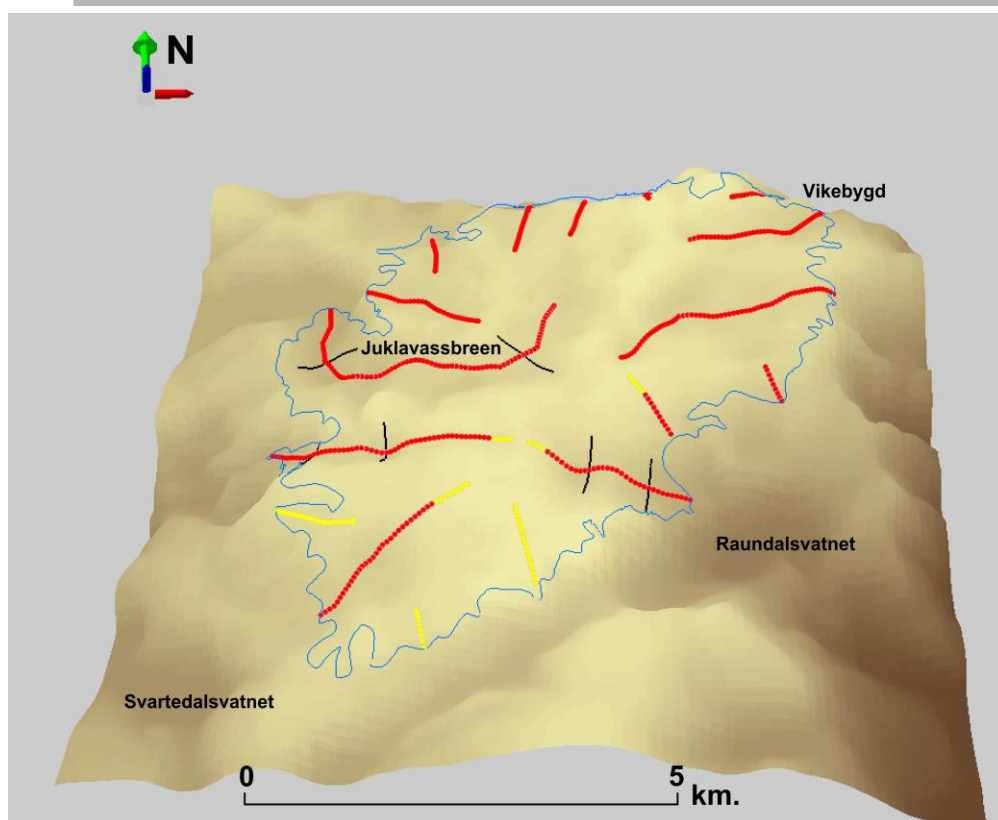
Figure 3. Reconstruction inputs for Folgefonna. The subglacial topography was retrieved from a ground penetrating radar survey. The blue line indicates the present-day ice margin, black lines are the cross-sections for F factor calculation red lines represent the flowlines. Red colour points have a predefined shear stress of 100 kPa and yellow colour points have a 50 kPa shear stress value.

Since both the ice surface and bed topography are known, it would be possible to tune the various tool parameters to fit the output of the glacier reconstruction tool to the present day glacier surface. However, the point of this exercise is to assess the quality of the reconstruction achievable replicating the situation where the icefield had disappeared and there were only ice geometry data available i.e. outlet glacier and plateau terminating moraines or precipitous plateau edges where ice avalanched off (Rea et al., 2000; Evans et al., 2002).

Shear stress along the flowlines was input in a very simple manner. For large icefields basal shear stresses tend towards zero near the central ice divide as ice surface slopes decrease. On the other hand, given the rough subglacial topography and thickness of Folgefonna, a "typical" 100 kPa shear stress value (Benn and Hulton, 2010) was applied along all flowlines with a few minor exceptions. Flowlines in the S and SE sectors had shear stresses reduced to 50 kPa to account for limited ice flow in this area. It is worth noting that for deglaciated plateau we would recommend reconstructing the moraine constrained outlet glaciers first. Then "tune" any flowlines, from the plateau margins where there are no moraines (needed to generate a complete icefield reconstruction), to fit where they meet the ice divides for the outlet glaciers (Evans et al., 2002). For the reasons outlined above portions of the flowlines near the central ice divide were assigned a shear stress of 50 kPa (see Figure 13). F factors have only been calculated for parts of flowlines where outlets were constrained within in a well-defined trough (i.e. along Juklavassbreen, Raundalsvatnet and its opposite outlet to the W).

Without use of F factors the reconstruction, as expected, underestimates ice thickness, and subsequently ice volumes, by about 25-30%. With the automatically derived F factor and subsequently the user-defined F factor the results improve considerably, but overall all reconstructions underestimate the volume and extension of ice to some extent (Table 1). This is mainly because there are areas far from the flowlines where the interpolation performs less well. This shortcoming could easily be overcome by using a denser flowline pattern, but we wished to test the tool using a minimum flow line configuration. Changes in volume and area are in general similar for the different interpolation methods, and, as expected, IDW and kriging yield the best results in volume and Trend the poorest (see section 2.3).

	Volume (km^3)	Volume difference (km^3)	Volume difference (%)	Area (km^2)	Area difference (km^2)	Area difference (%)
Extant glacier	2.80			27.48		
Model Topo to Raster	2.08	-0.72	-26	23.82	-3.66	-13
Model Topo to Raster w/ cross-sections	2.47	-0.33	-12	25.00	-2.48	-9
IDW w/cross-sections	2.57	-0.23	-8	24.82	-2.66	-10
Kriging w/cross-sections	2.58	-0.22	-8	24.95	-2.53	-9
Trend w/cross-sections	2.61	-0.19	-7	21.94	-5.54	-20

Table 1. Difference in volume and area between the model results and the extant Folgefonna.

The glacier-surface estimated ELA for the reconstructed icefield, which is arguably the most important use for palaeoglacier reconstructions, is very close to that of the extant glacier (Table 2). In particular, and whichever ELA methods and ratios are adopted (Pellitero et al., 2015), the difference in ELA between the reconstruction and real glacier is on the order of a few metres. The model with no F factor underestimates the ELA by ~15 metres, but the F factor model almost perfectly matches the real glacier ELA, with the error generally near that resulting from the contour belt elevation interval (see Pellitero et al., 2015), which was set to 5 metres for all reconstructions. It must be stressed that the extant glacier limit was used as input, so in this case there was no error in the horizontal geometry of the glacier reconstruction, as would likely be the case for the reconstruction of a fully deglaciated plateau.

	ELA MGE (m)	Difference (m)	ELA AA (m)	Difference (m)	ELA AAR 0.65 (m)	Difference (m)	ELA AABR 1.7 (m)	Difference (m)
Extant glacier	1518		1492		1468		1471	
Model Topo to	150	-17	147	-13	1466	-2	1459	-12

Raster	1		9					
Model Topo to Raster w/ cross-sections	1515	-3	1493	1	1480	12	1475	4
IDW w/cross-sections	1515	-3	1496	4	1475	7	1470	-1
Kriging w/cross-sections	1509	-9	1498	6	1479	11	1474	3
Trend w/cross-sections	1515	-3	1501	9	1485	17	1480	9

Table 2. Changes in ELA between the modelled glaciers and the extant Folgefonna, in meters. ELA methods detail can be found in Pellitero et al. (2015).
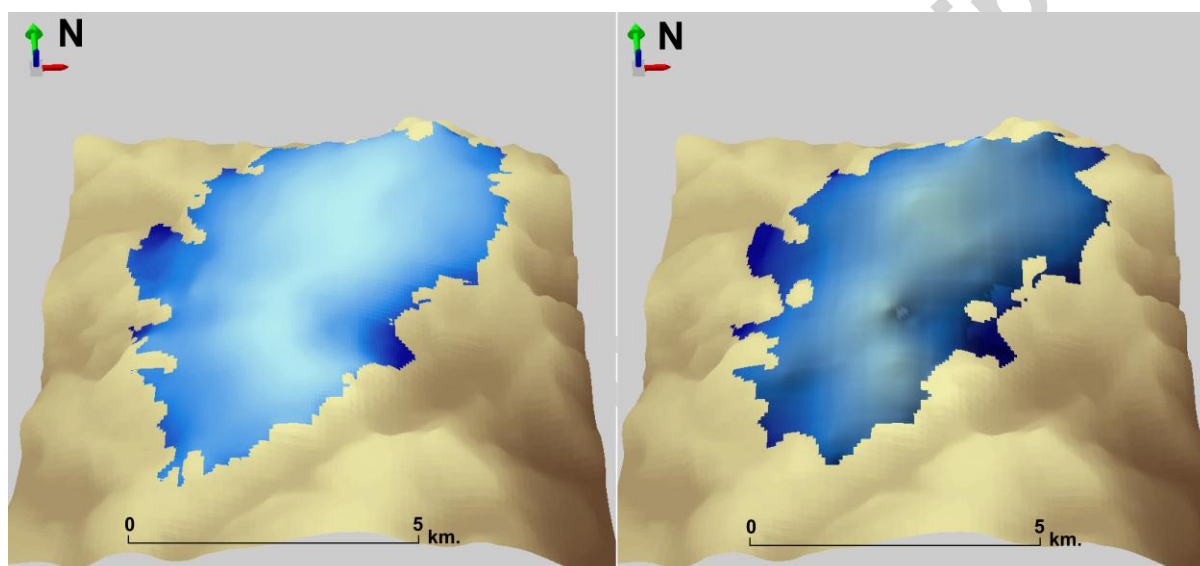

Figure 4. Comparison between the extant Folgefonna glacier (left) and the modelled glacier using Topo to Raster interpolation and the use of cross-sections as explained in the text (right).

Griesseglescher is a valley glacier in the Valais region of the Swiss Alps. The glacier flows from a large single cirque, whose peaks reach 3380 m.a.s.l., and has a total length of about 5 km. The glacier also has a branch that flows across a pass, to the south, into the Italian Val Formazza. The geometries and ELA calculation for the models and the present-day glacier are limited to the NE (Swiss) part of the glacier. The subglacial topography has been determined using surface slope and ice flux continuity, constrained by radio-echo sounding measurements along 14 cross profiles (Farinotti et al., 2009).

In this case the glacier limits are topographically-constrained so this serves as a good test to verify how accurately the planar extent of the glacier can be reconstructed. The upper portion of the subglacial topography has two tributary basins, so two flowlines which converge near the snout have been created (Figure 5). Three user-defined cross-sections were drawn where the subglacial topography indicates the development of significant troughs.
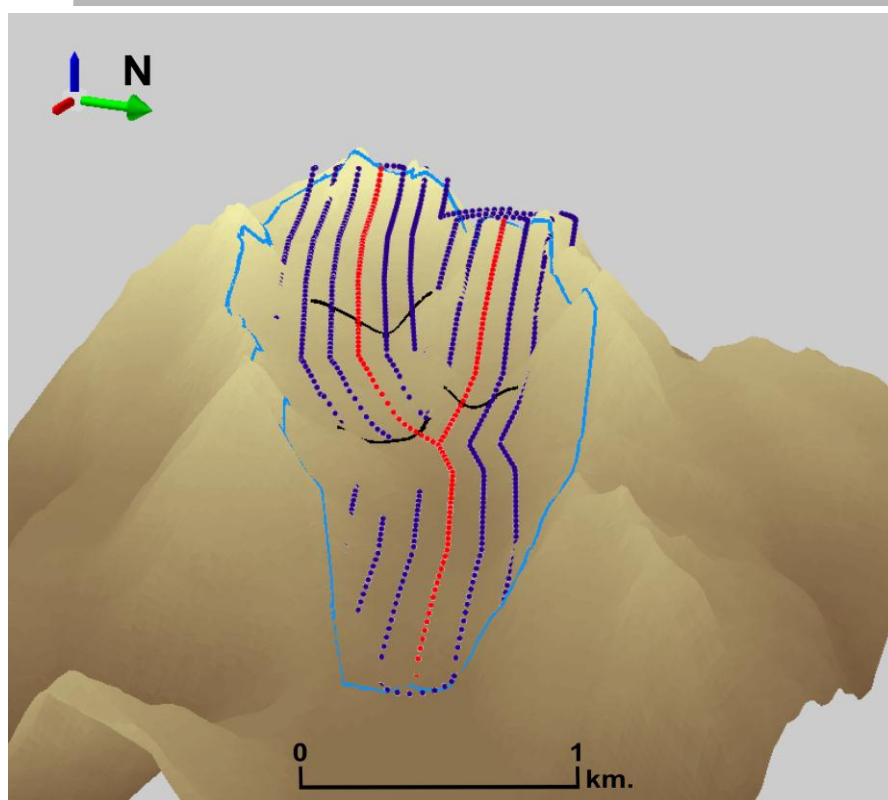
Figure 5. Subglacial topography at Griessglescher, with flowlines (red dots), catchment limit (blue line), cross-sections (black solid lines) and extended point ice surface network (blue dots), which were used in the glacier surface reconstruction.

In terms of surface area and volume, the models have variable results (Table 3). All the glacier reconstructions fall within a range of 25% error in volume and 20% in surface area. The highest errors result from running the tool with no F factor, because the drag effect is not accounted for (see section 2.2). Automatic F factor calculation reduces the error in volume to around 15%, whereas user defined cross-sections reduce the error to <10%. Result for the surface show a similar pattern, being 20% with no F factor, and ~6% when the F factor is considered. Again, the tool tends to slightly underestimate both volume and area.

	Volume (km^3)	Volume difference (km^3)	Volume difference %	Area (km^2)	Area difference (km^2)	Area difference (%)
Extant glacier	0.408			5.85		
Topo to raster	0.323	-0.086	-21	4.66	-1.18	-20
Topo to raster Auto cross-sections	0.480	0.071	17	5.49	-0.36	-6
Topo to raster User cross-sections	0.457	0.047	12	5.4	-0.45	-8
IDW	0.313	-0.095	-23	4.64	-1.21	-21
IDW Auto cross-sections	0.471	0.063	15	5.5	-0.35	-6
IDW User cross-	0.446	0.037	9	5.41	-0.43	-7

sections						
Kriging	0.316	-0.092	-22	4.65	-1.20	-21
Kriging Auto cross-sections	0.474	0.065	16	5.49	-0.36	-6
Kriging User cross-sections	0.449	0.041	10	5.41	-0.44	-8
Trend	0.314	-0.094	-23	4.64	-1.21	-2
Trend Auto cross-sections	0.468	0.06	15	5.46	-0.38	-7
Trend User cross-sections	0.437	0.029	7	5.42	-0.43	-7
RMS error (%)			16			10

Table 3. Area and surface volume comparison between the extant glacier and model results for Griesseglescher.

All reconstructions yielded a lower ELA than the real glacier-surface estimated ELA, most likely because the model underestimates the accumulation area. ELA errors are quite significant (~75 m.) when no shape factor is considered in the reconstruction. However, the error significantly decreases to 15-20 metres when the automated F factor tool is applied and down 10-15 metres when F factor calculation for user-defined cross-sections is implemented.

	ELA MEG (m)	Difference (m)	ELA AAA (m)	Difference (m)	ELA AAR 0.65 (m)	Difference (m)	ELA AABR 1.7	Difference (m)
Extant glacier	2927		2876		2817		2832	
Topo to raster	2844	-83	2821	-55	2684	-133	2778	-54
Topo to raster Auto cross-sections	2903	-24	2869	-7	2761	-56	2818	-14
Topo to raster User cross-sections	2911	-16	2875	-1	2773	-44	2826	-6
IDW	2846	-81	2822	-53	2696	-121	2771	-61

			3					
IDW Auto cross-sections	2906	-21	2873	-3	2786	-31	2821	-11
IDW User cross-sections	2916	-11	2880	4	2786	-31	2831	-1
Kriging	2845	-82	2825	-51	2695	-122	2780	-52
Kriging Auto cross-sections	2915	-12	2874	-2	2785	-32	2820	-12
Kriging User cross-sections	2915	-12	2881	5	2785	-32	2830	-2
Trend	2822	-105	2817	-59	2722	-95	2777	-55
Trend Auto cross-sections	2886	-41	2865	-11	2786	-31	2821	-11
Trend User cross-sections	2885	-42	2868	-8	2775	-42	2820	-12
RMS error (m)		44		22		64		24

Table 4. ELA comparison between the extant glacier and reconstructed Griesseglescher. All ELAs have been calculated using Pellitero et al. (2015)
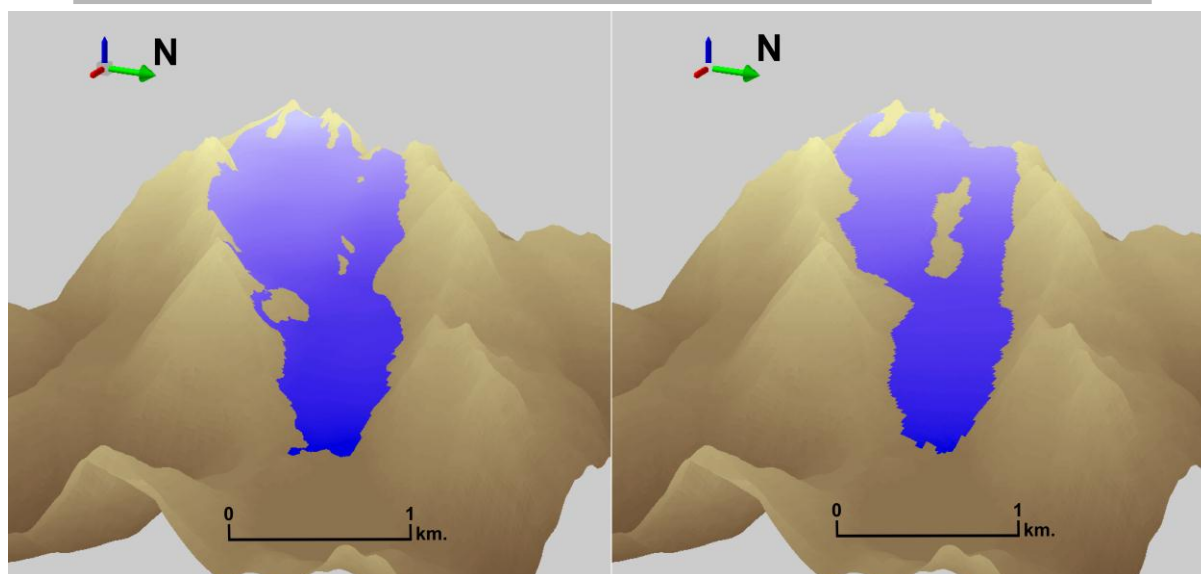
Figure 6. Comparison between the real Griesseglescher surface (left) and the one modelled with user-defined cross-sections (see Figure 15 and text) and IDW interpolation.

Figure 6 and Tables 3 and 4 show that the errors in the reconstruction are low when user-defined F-factors are used, and errors changed little from one interpolation method to other. This is because the extension of the central flowline ice surface elevation 600 m. sideways permitted the creation of a well distributed, dense network of ice surface elevation points, which minimizes the impact of the choice of interpolation method (see Figure 5). This situation is different to the Folgefonna glacier, where there were extensive areas with no ice thickness points nearby, so the reconstructed surface is more sensitive to the interpolation method.

Overall, the results from the two tests show that the reconstruction tool generated high quality results, bearing in mind that none of the glaciers used for testing are in present equilibrium with the climate, but demonstrates that multiple flowlines and the use of F factors for user-defined cross-sections is the best approach. In general, and regardless of the approach, one should never forget that the quality of a glacier 3D surface reconstruction is always related to the quality of the input parameters. Different input parameter requirements are also needed depending on the complexity of the glacier system under consideration. For example, a simple, topographically well-constrained valley palaeoglacier could be well reconstructed simply on the basis of the present-day topography and the position of a frontal moraine. More complex systems, such as an icefield with multiple outlets, ideally require a more extensive knowledge of the original glacier margins in order to obtain a robust reconstruction. For the purpose of testing the quality of the tool, we have assumed the ideal scenario where these inputs parameters are fully known (i.e. we used the known Folgefonna icefield margin) and demonstrated that the tool is able to reconstruct an icefield very similar to the present-day. We have demonstrated here that the tool is capable of providing robust, physically plausible reconstructions, but how well these reproduce any palaeoglacier ultimately depends on the quality of the input parameters, and in particular on the accurate mapping of the ice marginal geomorphology. This is where the expert knowledge of the glacial geomorphologist is paramount.

5. Conclusions.

The GlaRe toolbox implements a well-established approach for the determination of palaeoglacier equilibrium profiles. Significantly it allows users to quickly run multiple glacier reconstructions which were previously very laborious and time consuming (typically days for a single valley glacier). The GlaRe tool can be used to address at least two fundamental problems:

1. glacier reconstruction is crucial for the calculation of palaeoglacier ELAs and subsequent derivation of quantitative palaeoclimatic data. Reconstructions should be based on a rigorous interpretation of glacial landforms, as well as an assessment and testing of the reconstruction technique of the glacier surface and its physical plausibility. The tool presented here, because if its easy-to-use and straightforward approach, and the requirement of minimal inputs, is ideal to test different scenarios and glacier dynamic conditions.

2. the ability to run large numbers of reconstructions provides an opportunity to undertake palaeoglacier reconstructions across entire mountain ranges, regions or even continents, allowing climatic gradients and atmospheric circulation patterns to be elucidated.

Results from a comparison between extant glacier surfaces and modelled ones show very similar ELA values, on the order of 10-20 m error (which would account for a 0.065-0.13 °C variation using a typical -6.5 °C/100 m altitudinal lapse rate), and these can be improved further by increasing the number of flowlines and using F factors where appropriate. Overall, GlaRe has been demonstrated to be able to quickly generate robust palaeoglacier surfaces based on limited geomorphological inputs.

References

Bauder, A., Funk, M., Huss, M., 2007. Ice volume changes of selected glaciers in the Swiss Alps since the end of the 19th century. Ann. Glaciol., 46, 145-150.

Benn, D. I., Hulton, N.R.J., 2010. An ExcelTM spreadsheet program for reconstructing the surface profile of former mountain glaciers and ice caps. Comput. Geosci., 36, 605-610.

Braithwaite, R.J., 2008. Temperature and precipitation climate at the equilibrium line altitude of glaciers expressed by the degree-day factor for snow melting. J. Glaciol., 54, 437-444.

Carr, S.J., Lukas, S., Mills, S.C., 2010. Glacier reconstruction and mass-balance modelling as a geomorphic and palaeoclimatic tool. Earth Surf. Proc. Land., 35, 1103-1115.

Dahl, S. O., Nesje, A., 1992. Paleoclimatic implications based on equilibrium-line altitude depressions of reconstructed younger dryas and holocene cirque glaciers in inner Nordfjord, Western Norway. Palaeogeogr. Palaeoclimatol. Palaeoecol., 94 (1–4), 87–97.

Dawson, A.G., 1979. A Devensian Medial Moraine in Jura. Scottish J. Geol., 15, 43-48.

Evans, D.J.A., Rea, B.R., Hansom, J.D. and Whalley, W.B., 2002. The geomorphology and style of plateau icefield glaciation in a fjord terrain, Troms-Finnmark, north Norway. J. Quat. Sci., 17, 221-239.

Federici, P.R, Granger, D.E., Pappalardo, M., Ribolini, A., Spagnolo, M., Cyr, A.J., 2008. Exposure age dating and Equilibrium Line Altitude reconstruction of an Egesen moraine in the Maritime Alps, Italy. Boreas, 37, 245-253.

Farinotti, D., Huss, M., Bauder, A., Funk, M., Truffer, M., 2009. A method to estimate the ice volume and ice-thickness distribution of alpine glaciers. J. Glaciol., 55 (191), 422-430.

Hughes, P.D., Braithwaite, R.J., 2008. Application of a degree-day model to reconstruct Pleistocene glacial climates. Quaternary Res. 69, 110-116.

Huss, M., Bauder, A., Funk, M., 2009. Homogenization of long-term mass-balance time series. Ann. Glaciol., 50, 198-206.

Hutchinson, M.F., 1989. A new procedure for gridding elevation and stream line data with automatic removal of spurious pits. J. Hydrol., 106, 211-232.

Hutchinson, M.F., Xu, T., Stein, J.A., 2011. A recent progress in the ANUDEM elevation gridding procedure. In: Hengl T., Evans I., Wilson J. and Gould M. (Eds.), Geomorphometry 2011, Redlands, California, USA, 19–22.

Li, H., Ng, F., Li, Z., Qin, D., Cheng, G., 2012. An extended "perfect-plasticity" method for estimating ice thickness along the flow line of mountain glaciers. J. Geophys. Res., 117 (F1), 2156-2202.

Lukas, S., 2006. Morphostratigraphic principles in glacier reconstruction – a perspective from the British Younger Dryas. Prog. Phys. Geog., 30 (6), 719-736.

Nye, J. F., 1952a. A method of calculating the thicknesses of the ice-sheets, Nature, 169, 529-530.

Nye, J.F., 1952b. The Mechanics of Glacier Flow. J. Glaciol., 2, 82-93.

Nye, J.F., 1965. The flow of a glacier in a channel of rectangular, elliptic or parabolic cross-section. J. Glaciol., 5. 661-690.

Ohmura, A., Kasser, P., Funk, M., 1992. Climate at the equilibrium line of glaciers. J. Glaciol., 38 (130), 397-411.

Oliver, M.A., Webster, R., 2014. A tutorial guide to geostatistics: Computing and modelling variograms and kriging. CATENA, 113: 56-69.

Paterson, W.S.B., 1970. The sliding velocity of Athabasca glacier, Canada. J. Glaciol., 9 (55), 55-63.

Paterson, W.S.B., 1994. The Physics of Glaciers. 3rd Edition. Pergamon/Elsevier, London.

Pellitero, R., 2013. Lateglacial evolution of Fuentes Carrionas massif (Cantabrian Range), palaeoenvironmental and chronological estimations. Cuatern. Geomorfol., 27 (1-2), 71-90.

Pellitero, R., Rea, B., Spagnolo, M. Bakke, J., Hughes, P., Ivy-Ochs, S., Lukas, S., Ribolini, A., 2015. A GIS tool for automatic calculation of glacier equilibrium-line altitudes. Comput. Geosci. 82, 55-62.

Rea, B.R., Whalley, W.B., Dixon, T., Gordon, J.E., 1999. Plateau icefields as contributing areas to valley glaciers and the potential impact on reconstructed ELAs: a case study from the Lyngen Alps, North Norway. Ann. Glaciol., 28, 97-102.

Rea, B.R., Evans, D.J.A., 2007. Quantifying climate and glacier mass balance in north Norway during the YD. Palaeogeogr. Palaeoclimatol. Palaeoecol., 246, 307-330.

Shilling, D.H., Hollin, J.T., 1981. Numerical reconstructions of valley glaciers and small ice caps. In: Denton, G.H., Hughes, T.J. (Eds.), The Last Great Ice Sheets. Wiley, New York, pp. 207-220.

Tobler, W., 1970. A computer movie simulating urban growth in the Detroit region. Econ. Geogr., 46(2): 234-240.

Van der Veen, C.J., 2013. Fundamentals of Glacier Dynamics. 2nd edition. Balkema, Rotterdam.

Weertman, J., 1971. Shear stress at the base of a rigidly rotating cirque glacier. J. Glaciol., 10 (58), 31-37.

Highlights

- GlaRe is a tool for palaeoglacier 3D surface reconstruction from bed topography.
- GlaRe is coded in Python and runs in ArcGIS as a toolbox.
- The theory of perfect plasticity equilibrium glacier profile is considered.
- Interpolation methods for glacier 3D surface creation are described and discussed.
- Glare is tested with two extant glaciers, showing a small, acceptable error.